THE UNIVERSITY *of* EDINBURGH

# Edinburgh Research Explorer

## Underground experimental study finds no evidence of low-energy resonance in the 6Li(p,γ)7Be reaction

OPEN ACCESS

# Underground experimental study finds no evidence of low-energy resonance in the $^6$Li($p,\gamma$)$^7$Be reaction

D. Piatti,[1] T. Chillery,[2] R. Depalo,[1, *] M. Aliotta,[2] D. Bemmerer,[3] A. Best,[4] A. Boeltzig,[5] C. Broggini,[6] C.G. Bruno,[2] A. Caciolli,[1] F. Cavanna,[7] G.F. Ciani,[5] P. Corvisiero,[7] L. Csedreki,[5] T. Davinson,[2] A. Di Leva,[4] Z. Elekes,[8] F. Ferraro,[7] E.M. Fiore,[9] A. Formicola,[10] Zs. Fülöp,[8] G. Gervino,[11] A. Gnech,[12] A. Guglielmetti,[13] C. Gustavino,[14] Gy. Gyürky,[8] G. Imbriani,[4] M. Junker,[10] I. Kochanek,[10] M. Lugaro,[15] L.E. Marcucci,[16] P. Marigo,[17] E. Masha,[13] R. Menegazzo,[6] V. Mossa,[9] F.R. Pantaleo,[9] V. Paticchio,[18] R. Perrino,[18] P. Prati,[7] L. Schiavulli,[9] K. Stöckel,[19] O. Straniero,[20] T. Szücs,[3] M.P. Takács,[19] and S. Zavatarelli[7]

(LUNA collaboration)

[1] *Università degli Studi di Padova and INFN, Sezione di Padova, 35131 Padova, Italy*
[2] *SUPA, School of Physics and Astronomy, University of Edinburgh, EH9 3FD Edinburgh, United Kingdom*
[3] *Helmholtz-Zentrum Dresden-Rossendorf, 01328 Dresden, Germany*
[4] *Università degli Studi di Napoli "Federico II" and INFN, Sezione di Napoli, 80126 Napoli, Italy*
[5] *Gran Sasso Science Institute, 67100 L'Aquila, Italy and INFN,*
*Laboratori Nazionali del Gran Sasso, 67100 Assergi, Italy*
[6] *INFN, Sezione di Padova, 35131 Padova, Italy*
[7] *Università degli Studi di Genova and INFN, Sezione di Genova, 16146 Genova, Italy*
[8] *Institute for Nuclear Research (Atomki), PO Box 51, 4001 Debrecen, Hungary*
[9] *Università degli Studi di Bari, Dipartimento Interateneo di Fisica, 70125 Bari, Italy*
*and INFN, Sezione di Bari, 70125 Bari, Italy*
[10] *INFN, Laboratori Nazionali del Gran Sasso (LNGS), 67100 Assergi, Italy*
[11] *Università degli Studi di Torino and INFN, Sezione di Torino, 10125 Torino, Italy*
[12] *Gran Sasso Science Institute, 67100 L'Aquila, Italy and INFN, Sezione di Pisa, 56127 Pisa, Italy*
[13] *Università degli Studi di Milano and INFN, Sezione di Milano, 20133 Milano, Italy*
[14] *INFN, Sezione di Roma, 00185 Roma, Italy*
[15] *Konkoly Observatory, Research Centre for Astronomy and Earth Sciences, 1121 Budapest, Hungary*
*and ELTE Eötvös Loránd University, Institute of Physics, 1117 Budapest, Hungary*
[16] *Dipartimento di Fisica, Università degli Studi di Pisa and INFN, Sezione di Pisa, 56127 Pisa, Italy*
[17] *Università di Padova, Dipartimento di Fisica e Astronomia, 35131 Padova, Italy*
[18] *INFN, Sezione di Bari, 70125 Bari, Italy*
[19] *Helmholtz-Zentrum Dresden-Rossendorf, 01328 Dresden, Germany*
*and Technische Universität Dresden, Institut für Kern- und Teilchenphysik, 01069 Dresden, Germany*
[20] *INFN, Laboratori Nazionali del Gran Sasso (LNGS), 67100 Assergi, Italy*
*and INAF Osservatorio Astronomico d'Abruzzo, 64100 Teramo, Italy*

The astrophysical $^6$Li($p,\gamma$)$^7$Be reaction occurs during Big Bang nucleosynthesis and the pre-main sequence and main sequence phases of stellar evolution. The low-energy trend of its cross section remains uncertain, since different measurements have provided conflicting results. A recent experiment reported a resonance-like structure at center-of-mass energy 195 keV, associated to a positive-parity state of $^7$Be. The existence of such resonance is still a matter of debate. We report a new measurement of the $^6$Li($p,\gamma$)$^7$Be cross section performed at the Laboratory for Underground Nuclear Astrophysics, covering the center-of-mass energy range $E$ = 60 - 350 keV. Our results rule out the existence of low-energy resonances. The astrophysical $S$-factor varies smoothly with energy, in agreement with theoretical models.

*Introduction* − The abundance of lithium in the Universe is a complex topic involving all three main nucleosynthesis scenarios: Big Bang Nucleosynthesis (BBN), the interaction of cosmic rays with interstellar matter, and stellar nucleosynthesis [1]. Detailed simulations of the chemical evolution of the Galaxy [2] have shown that less than half of the solar system lithium was produced by BBN [3, 4] or Galactic cosmic rays, with the remainder to be supplied by low-mass stellar sources such as red giants, asymptotic giant branch stars, or novae [2].

BBN lithium production is dominated by the $^2$H($\alpha,\gamma$)$^6$Li [5, 6] and $^3$He($\alpha,\gamma$)$^7$Be [7] reactions for its two stable isotopes $^{6,7}$Li, respectively. The predicted BBN $^6$Li/$^7$Li isotopic ratio is $10^{-4}$ [5, 7], much lower than the solar system value of 0.08 [8]. Similarly, very low $^6$Li/$^7$Li values are also expected for low-mass stellar lithium sources. The same is true for neutrino nucleosynthesis, which may provide significant amounts of $^7$Li but not $^6$Li [9]. In contrast, the $^6$Li/$^7$Li production ratio in Galactic or structure formation cosmic rays is much higher, close to unity [10].

The so-called Spite plateau of $^7$Li abundances in metal-poor stars [11] is 2-4 times below the predicted BBN abundance [3], a discrepancy known as the cosmological lithium problem [12, 13]. Stellar solutions to this problem are under discussion [14, 15], but the recent observa-

tion of lithium close to the Spite plateau in an extremely metal-poor star seems to reinforce the lithium problem [16]. In this context, it has been suggested to use the $^6$Li/$^7$Li isotopic ratio as a tool to constrain non-standard lithium production mechanisms [2, 17] and pollution of stellar atmospheres [18].

While the $^6$Li$(p,\alpha)^3$He reaction easily depletes $^6$Li in stars, the competing but much slower $^6$Li$(p,\gamma)^7$Be reaction may convert some $^6$Li to $^7$Li (the daughter of radioactive $^7$Be), which is less readily destroyed in stars, thus affecting both the numerator and the denominator of the $^6$Li/$^7$Li ratio.

The cross section of the $^6$Li$(p,\alpha)^3$He reaction is known to 5% precision at the energies of astrophysical interest [19, 20]. On the other hand, the low-energy behavior of the $^6$Li$(p,\gamma)^7$Be cross section is still poorly understood, despite theoretical and experimental efforts. Previous low-energy measurements of the $^6$Li$(p,\gamma)^7$Be cross section at center-of-mass energies below 200 keV have given conflicting results on the slope of the astrophysical $S$-factor. Three data sets are available in the literature: the first measurement of the $^6$Li$(p,\gamma)^7$Be cross section relative to the $^6$Li$(p,\alpha)^3$He at center-of-mass energies between 40 and 150 keV led to a positive slope of the $S$-factor (Cecil *et al.* [21]). A subsequent measurement of the energy dependence of the $^6$Li$(p,\gamma)^7$Be $S$-factor at proton beam energies between 80 and 130 keV found a negative slope (Prior *et al.* [22]). The most recent cross section measurement by He *et al.* [23] reported instead a positive slope of the $S$-factor, in qualitative agreement with [21], which was interpreted either as a possible novel reaction mechanism or as a new resonance at center-of-mass energy of 195 keV. In order to reproduce their experimental data, He *et al.* assumed the presence of an excited state in $^7$Be with $E_x \approx 5800$ keV, $J^\pi = (1/2^+, 3/2^+)$ and $\Gamma_p \approx 50$ keV in their R-matrix calculation [23]. This claim is indirectly supported by the measured $^6$Li$(p,\alpha)^3$He angular distribution. In fact, while the $^6$Li$(p,\alpha)^3$He cross section shows no evidence of resonances around 200 keV [20, 24], its angular distribution is well-studied [25, 26, and references therein] and shows a prominent $A_1$ coefficient leading to the hypothesis of positive-parity states in $^7$Be [25, 27, 28].

The new $^7$Be excited state can potentially contribute as a resonance in the $^3$He$(^4$He$,\gamma)^7$Be reaction at center-of-mass energy $E \approx 4210$ keV and affect the extrapolation of the cross section to solar energies. However, a recent $^3$He$(^4$He$,\gamma)^7$Be cross section measurement found no evidence for such resonance [29].

From a nuclear structure point of view, the claimed resonance [23] is particularly intriguing because of its reported positive parity. There are no positive-parity $^7$Be states listed in the Evaluated Nuclear Structure Data [30]. In addition, the energy spectrum of mass-7 nuclei can now be calculated *ab initio* [31, 32], and such an excited state, if confirmed, would constrain such cal-

culations.

A number of theoretical calculations of the $^6$Li$(p,\gamma)^7$Be $S$-factor have been performed using different types of models [33–41]. None of them is able to reproduce the newly-reported resonance, unless this is added *ad-hoc* to reproduce the experimental data [36, 42]. Moreover, a recent no-core-shell-model calculation predicts only negative parity states up to 9 MeV excitation energy [43], corresponding to $E \approx 4$ MeV in the $^6$Li$(p,\gamma)^7$Be system.

To assess the low-energy trend of the $^6$Li$(p,\gamma)^7$Be $S$-factor, we performed a new experiment at the Laboratory for Underground Nuclear Astrophysics (LUNA), located at Laboratori Nazionali del Gran Sasso (Italy) [44, 45]. The deep-underground location guarantees an environmental background level orders of magnitude lower than above ground [44, 46], allowing to perform high-sensitivity measurements.

*Experimental setup and data acquisition* − A schematic view of the experimental setup is shown in Fig. 1. A high-intensity proton beam with energy rang-
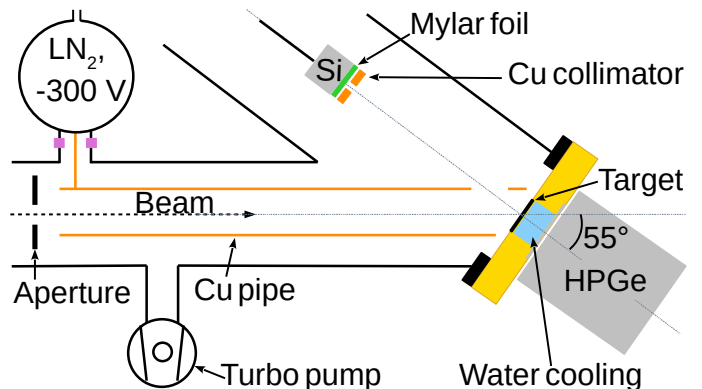


FIG. 1. Sketch of the experimental setup used for the measurement of the $^6$Li$(p,\gamma)^7$Be cross section at LUNA.

ing from 80 keV to 400 keV was provided by the LUNA-400 kV accelerator [47]. The beam was analyzed, collimated by a circular aperture of 0.3 cm diameter and sent through a 70 cm long copper pipe of 2.6 cm diameter. The copper pipe extended to a distance of 1 cm from the target and had a dual function: it was cooled to liquid nitrogen temperature to serve as a cold trap, and it was biased to $-300$ V for secondary electron suppression. The beam impinged on a $^6$Li-enriched solid target, tilted at $55°$ with respect to the beam direction. Targets were produced at Atomki (Hungary) by evaporation on tantalum disks (of thickness 0.25 mm and diameter 42 mm) previously cleaned with an acid bath. Three targets (of thicknesses $100 - 200$ $\mu$g/cm$^2$) were made using $^6$Li$_2$WO$_4$ powder from Sigma Aldrich; one target (thickness 20 $\mu$g/cm$^2$) was made using $^6$Li$_2$O powder produced at INFN - Legnaro National Laboratories (Italy) from metallic $^6$Li. The $^6$Li isotopic enrichment level was 95% for all targets. To limit target degradation, the target

backing was directly cooled by recirculating water.

The scattering chamber and the target were electrically insulated from the beam line and functioned as a Faraday cup for beam current measurements. Throughout the experiment a typical beam current of 100 $\mu$A was delivered on target.

The $^6$Li$(p,\gamma)^7$Be reaction ($Q$-value = 5607 keV) proceeds through direct capture (DC) to either the ground state of $^7$Be, or its first excited state, with subsequent emission of a 429 keV secondary gamma ray. Gamma rays were detected using a High-Purity Germanium detector (HPGe) of 104% relative efficiency [48] positioned at 1.7 cm from the target and at 55° with respect to the beam direction.

The absolute gamma-ray detection efficiency was measured using point-like radioactive sources ($^{137}$Cs, $^{60}$Co and $^{88}$Y), with activities calibrated by the Physikalisch-Technische Bundesanstalt (PTB) to 1% accuracy. The efficiency curve was then extended up to 6.8 MeV using the well-known $^{14}$N$(p,\gamma)^{15}$O resonance at proton energy $E_p$ = 278 keV [49, 50]. True coincidence summing effects [48] up to 16% were corrected using two independent approaches: an analytical correction [51, 52], and a Geant4 [53] simulation of the experimental setup [54, 55]. The results provided by the two methods are consistent within 4%. The simulation was also used to correct for true coincidence summing effects on the detected gamma-ray peak areas from $^6$Li$(p,\gamma)^7$Be transitions.

In addition to the HPGe detector, a silicon detector with 25 mm$^2$ active area and 100 $\mu$m depletion depth was installed at 125° from the beam direction, on a linear actuator. With this setup, the $\alpha$ and $^3$He particles from the $^6$Li$(p,\alpha)^3$He reaction were detected concurrently with the gamma rays from the $^6$Li$(p,\gamma)^7$Be reaction. The silicon detector was collimated by a 1 mm thick and 1 mm diameter aperture and shielded against elastically scattered beam particles by a 5 $\mu$m-thick Mylar foil. $\alpha$ and $^3$He particles could be clearly distinguished by reaction kinematics.

The charged-particle detection efficiency was measured using the $^{18}$O$(p,\alpha)^{15}$N resonance at $E_p$ = 151 keV, $\omega\gamma = (164.2^{+12.1}_{-11.7})$ meV [56, 57]. With this approach, the detection efficiency was determined in the same geometrical configuration adopted for the $^6$Li$(p,\alpha)^3$He measurement, with the main systematic uncertainty coming from the uncertainty on the $\omega\gamma$ of the resonance used.

An additional source of uncertainty on both particle and gamma-ray detection efficiency was due to the relative geometry of the beam spot and the detector. The effect is more pronounced for the Si detector, since the diameter of the collimator ($\phi_{Si}$ = 1 mm) was much smaller than the beam spot on target ($\phi_{beam} \approx$ 10 mm) [58]. The uncertainty due to the source-to-detector geometry was estimated using a simulation in which the beam spot was located at different positions, in accordance with observed beam spots on target. The effect was found to be

5% for the Si detector and 2% for the HPGe detector.

*Data analysis* – A measurement of the $^6$Li$(p,\gamma)^7$Be and $^6$Li$(p,\alpha)^3$He excitation functions in the whole dynamic range of the LUNA-400 kV accelerator was performed for each target. In this way it was possible to make consistency checks between different data sets and verify that our results are unaffected by systematic effects due to target composition and thickness. In each run, the gamma-ray and charged-particle spectra were recorded simultaneously and stored for off-line analysis. The $^6$Li$(p,\gamma)^7$Be experimental yield was given by the sum of the contributions from the direct capture to the ground state ($\gamma_0$) and to the 429 keV excited state ($\gamma_1$) of $^7$Be. Fig. 2 shows the ratio of the two transition probabilities compared to the literature. The effect of gamma-ray angular distribution was taken into account in the present evaluation of the transition probabilities (more details on the angular distributions adopted are provided in the next paragraphs). As a result, the ratio B($\gamma_0$)/B($\gamma_1$) is observed to slightly increase with energy. The average branching ratio from the present experiment is 1.72 $\pm$ 0.11 (red line in Fig. 2), in good agreement with literature values [22, 23, 59].
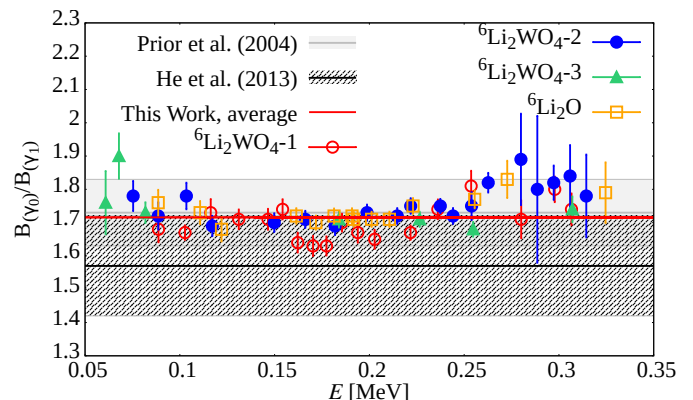


FIG. 2. Ratio of the counting rates in the DC→0 ($\gamma_0$) and DC→429 keV ($\gamma_1$) for each target, corrected for detection efficiency and angular distribution. The ratio is compared to literature values [22, 23]. Shaded areas represent the uncertainties on literature values. The present error bars reflect only the statistical uncertainties.

For the calculation of the $^6$Li$(p,\gamma)^7$Be $S$-factor, we adopted a relative approach: the $(p,\gamma)$ cross section was normalized at each energy to the literature $(p,\alpha)$ cross section [20]. At any given beam energy, the ratio of the experimental yields for the $\gamma$ ($Y_\gamma$) and $\alpha$ ($Y_\alpha$) channels is given by:

$$\frac{Y_\gamma}{Y_\alpha} = \frac{N_\gamma}{N_\alpha} \cdot \frac{\eta_\alpha W_\alpha(\theta)}{\eta_\gamma W_\gamma(\theta)} \qquad (1)$$

where $N$ is the net (i.e. background-subtracted) number of gamma or alpha peak counts observed in the
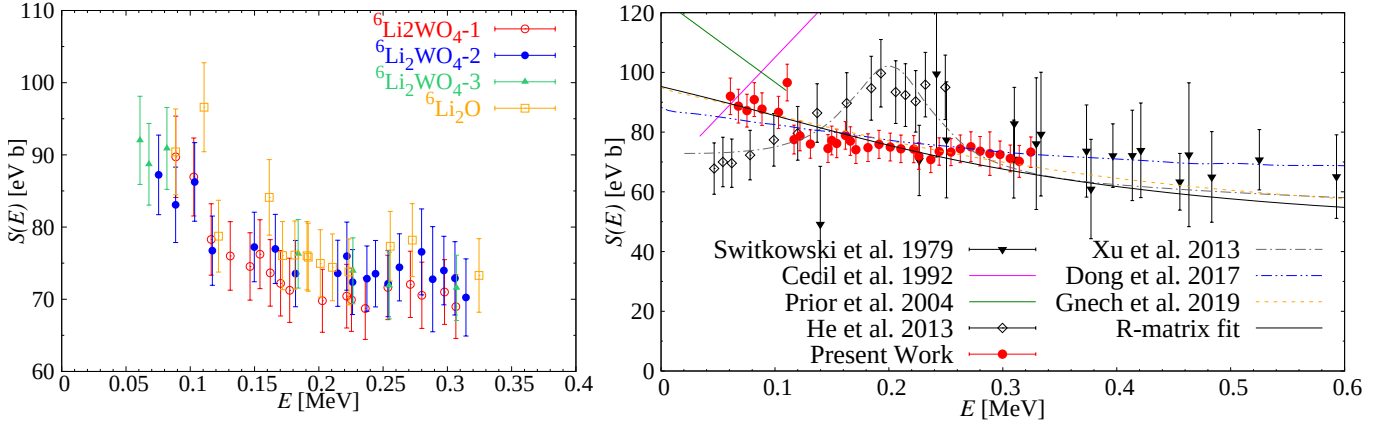
FIG. 3. Astrophysical $S$-factor for the $^6$Li$(p,\gamma)^7$Be reaction as obtained from individual targets (left panel) and from a weighted average of the different datasets (red filled circles, right panel). Previous experimental data and theoretical evaluations are also shown for comparison in the right panel. The solid black line represents an R-matrix fit of present data and data from [59].

spectrum, $\eta$ the detection efficiency, and $W(\theta) = 1 + \sum_{k=1}^{N} A_k P_k(\cos(\theta))$ the angular distribution correction factor, with $P_k(\cos(\theta))$ being the Legendre polynomial of order $k$. The subscripts $\gamma$ and $\alpha$ refer to the $(p,\gamma)$ and $(p,\alpha)$ channels, respectively. For the $(p,\alpha)$ channel, the angular distribution coefficients $A_k$ and related uncertainties were taken from [25, 26, 60]. For the $(p,\gamma)$ channel, no angular distribution measurements are available in the literature for the energy range explored in the present study. Therefore, we adopted a theoretical angular distribution using the model described in [40]. For the resultant uncertainty, we repeated the analysis, first, using an anisotropy twice as large as given in Ref. [40], and second, assuming isotropy [61]. The only other theoretical angular distributions available [33] fall in this range. Due to the position of the detector, its close proximity to the target and the relatively mild anisotropy (the first to third order Legendre coefficients were between 0.0-0.2 [40]), the effect on the gamma-ray detection efficiency is ≤3%.

At each energy, the ratio of the two yields can be expressed in terms of the astrophysical $S$-factors for the $\gamma$ ($S_\gamma$) and $\alpha$ ($S_\alpha$) channels as [62, 63]:

$$\frac{Y_\gamma}{Y_\alpha} = \frac{\int_{E_p - \Delta E_p}^{E_p} E^{-1} S_\gamma(E) e^{-2\pi\eta} \epsilon_{\text{eff}}^{-1}(E) dE}{\int_{E_p - \Delta E_p}^{E_p} E^{-1} S_\alpha(E) e^{-2\pi\eta} \epsilon_{\text{eff}}^{-1}(E) dE} \quad (2)$$

where $E_p$ is the proton beam energy, $\Delta E_p$ the energy lost by the beam inside the target (between 30 and 100 keV, depending on the type of target and on the beam energy), $\epsilon_{\text{eff}}(E)$ the effective stopping power, and $e^{-2\pi\eta}$ the Gamow factor [62]. The energy associated to each point is the cross-section-weighted average as defined in [64]. This approach to derive the $S$-factor is only weakly dependent on the target properties and behavior during

intense beam irradiation, as well as on the charge integration on target.

For normalization purposes, we adopted the parametrization of the $^6$Li$(p,\alpha)^3$He $S$-factor from [20] provided in [65], which reproduces experimental data in [20] to better than 1%. The energy dependence of the $S$-factor was taken into account both for the $\alpha$ and $\gamma$ channels: while $S_\alpha(E)$ is known, for $S_\gamma(E)$ the analysis was repeated assuming three different energy trends from Refs. [22, 23, 40]. Results were insensitive to the specific trend assumed.

The measured $S$-factors were finally corrected for electron screening, using the adiabatic approximation [66] and a screening potential $U_e = 273$ eV [20]. The screening correction amounted to at most 2.5%.

*Results and discussion* − The bare $S$-factor (i.e., the $S$-factor corrected for the electron screening effect) for the $^6$Li$(p,\gamma)^7$Be reaction from the present experiment is shown in Fig. 3, together with previous literature data and theoretical calculations. As shown in Fig. 3 all targets gave consistent results, therefore we adopted a weighted average of the different data-sets. A table with average S-factor values is provided as supplementary material [67]. The error bars in Fig. 3 account for statistical uncertainties (≤ 2%) and the uncertainty due to the relative geometry of the beam spot and the two detectors (6%). In addition, results are affected by a systematic error of 13%, due to the remaining uncertainty on charged-particle (8%) and gamma-ray (4%) detection efficiency, $^6$Li$(p,\alpha)^3$He $S$-factor (5%) and uncertainties on $W_\gamma(\theta)$ (3%) and $W_\alpha(\theta)$ (≤ 4%).

Our data have a monotonic dependence on the energy and show no evidence of the resonance reported by He *et al.* [23]. One point at 110.7 keV is observed to scatter with respect to the neighboring points. However, this deviation is observed only in one point. Moreover, if the uncertainty due to the beam spot position with respect

to the two detectors is taken into account, the point is still consistent with the trend drawn by the other points within two standard deviations. Fig. 3 also shows a simple R-matrix fit of our data and the data from Switkowski *et al.* [59], performed with the AZURE code [68]. The fit considers only the proton and gamma channels and is dominated by non-resonant capture. This is modelled with an external capture width to the ground state, plus two background poles with $J^\pi = 1/2^+$ and $1/2^-$ (proton orbital angular momentum $l_p = 0$ and 1, respectively) at $E_x = 20$ MeV. A more comprehensive fit including additional entrance channels, as well as a wider selection of data sets, is beyond the scope of this work. The fit provides an extrapolated S-factor to zero energy of $S(0) = 95 \pm 9$ eV b. This value is 30% higher than the extrapolation from [36], $S(0) = 73^{+56}_{-11}$ eV b, which includes the hypothetical 195 keV resonance. Our $S(0)$ is in very good agreement with the theoretical values from [40] ($S(0) = 95.0$ eV b, not renormalized) and [35] ($S(0) = 99.5$ eV b).

We used our new data in combination with those reported in [59] to evaluate the astrophysical reaction rate for the $^6$Li$(p,\gamma)^7$Be reaction, following the approach suggested in the NACRE compilation [69] for non-resonant cross sections. The new reaction rate, expressed as the Maxwellian-averaged $\langle \sigma v \rangle$ multiplied by the Avogadro number $N_A$ [62], is shown in Fig. 4, normalized to the reaction rate from the NACRE compilation [69]. Our recommended rate is consistent with the NACRE rate [69], while the uncertainty has been reduced by about a factor of 2. The rate from the NACRE II compilation [36] is also shown for comparison, where the recommended value was calculated assuming the existence of the 195 keV resonance, while for the upper limit the resonance was disregarded.
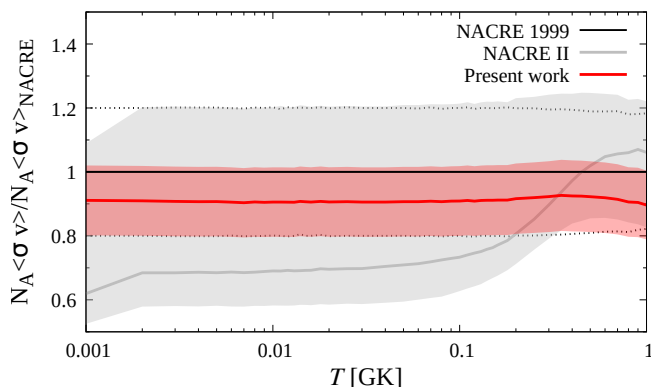


FIG. 4. Astrophysical reaction rate for the $^6$Li$(p,\gamma)^7$Be reaction, normalized to the NACRE rate [69]. The NACRE II rate [36] is also shown for comparison. Dashed lines represent the uncertainty on the NACRE rate, while shaded areas represent the uncertainties from the present experiment (red) and from NACRE II (grey).

In conclusion, the $^6$Li$(p,\gamma)^7$Be cross section has been measured at LUNA relative to the $^6$Li$(p,\alpha)^3$He cross section in the energy range from $60 - 350$ keV with $\leq 2\%$ statistical and 12% systematic uncertainty. A previously reported [23] possible resonance is ruled out by our new data. These new data provide a solid experimental reference for future *ab-initio* evaluations of reactions involving $^7$Be [31, 32].

The new thermonuclear reaction rate is 9% lower than NACRE [69] and 33% higher than reported in NACRE II [36] at 2 MK, and the reaction rate uncertainty has been significantly reduced. This will allow a more precise evaluation of the impact of the $^6$Li$(p,\gamma)^7$Be reaction on the lithium isotopic ratio in various stellar scenarios [2, 17, 70, 71].

* rdepalo@pd.infn.it
[1] J. A. Johnson, Science **363**, 474 (2019).
[2] N. Prantzos, Astron. Astrophys. **542**, A67 (2012).
[3] C. Pitrou *et al.*, Phys. Rep. **754**, 1 (2018).
[4] B. D. Fields *et al.*, J. Cosmol. Astropart. Phys. **2020**, 010 (2020).
[5] M. Anders *et al.*, Phys. Rev. Lett. **113**, 042501 (2014).
[6] D. Trezzi *et al.*, Astropart. Phys. **89**, 57 (2017).
[7] D. Bemmerer *et al.*, Phys. Rev. Lett. **97**, 122502 (2006).
[8] K. Lodders, Astrophys. J. **591**, 1220 (2003).
[9] A. Sieverding *et al.*, Astrophys. J. **876**, 151 (2019).
[10] B. D. Fields and T. Prodanović, Astrophys. J. **623**, 877 (2005).
[11] L. Sbordone *et al.*, Astron. Astrophys. **522**, A26 (2010).
[12] B. D. Fields, Annu. Rev. Nucl. Part. Sci. **61**, 47 (2011).
[13] M. Tanabashi *et al.*, Phys. Rev. D **98**, 030001 (2018).
[14] A. J. Korn *et al.*, Nature **442**, 657 (2006).
[15] Conference Lithium in the Universe: To Be or not to Be? (2019).
[16] D. S. Aguado *et al.*, Astrophys. J. Lett. **874**, L21 (2019).
[17] J. C. Howk *et al.*, Nature **489**, 121 (2012).
[18] G. Harutyunyan *et al.*, Astron. Astrophys. **618**, A16 (2018).
[19] J. Cruz *et al.*, Phys. Lett. B **624**, 181 (2005).
[20] J. Cruz *et al.*, J. Phys. G Nucl. Partic. **35**, 014004 (2008).
[21] F. Cecil *et al.*, Nucl. Phys. A **539**, 75 (1992).
[22] R. M. Prior *et al.*, Phys. Rev. C **70**, 055801 (2004).
[23] J. He *et al.*, Phys. Lett. B **725**, 287 (2013).
[24] L. Lamia *et al.*, Astrophys. J. **768**, 65 (2013).

[25] S. Engstler *et al.*, Z. Phys. A **342**, 471 (1992).

[26] C. Brune *et al.*, Nucl. Instrum. Methods Phys. Res., Sect. A **389**, 421 (1997).

[27] R. Bouchez *et al.*, J. Phys. Radium **21**, 346 (1960).

[28] F. Barker, Nucl. Phys. A **707**, 277 (2002).

[29] T. Szücs *et al.*, Phys. Rev. C **99**, 055804 (2019).

[30] D. Tilley *et al.*, Nucl. Phys. A **708**, 3 (2002).

[31] T. Neff, Phys. Rev. Lett. **106**, 042502 (2011).

[32] J. Dohet-Eraly *et al.*, Phys. Lett. B **757**, 430 (2016).

[33] F. Barker, Aust. J. Phys. **33**, 159 (1980).

[34] O. Camargo *et al.*, Phys. Rev. C **78**, 034605 (2008).

[35] J. Huang *et al.*, Atom. Data Nucl. Data **96**, 824 (2010).

[36] Y. Xu *et al.*, Nucl. Phys. A **918**, 61 (2013).

[37] K. Arai *et al.*, Nucl. Phys. A **699**, 963 (2002).

[38] A. Nesterov *et al.*, Ukr. J. Phys. **56**, 645 (2011).

[39] S. B. Dubovichenko *et al.*, Phys. At. Nucl. **74**, 984 (2011).

[40] A. Gnech and L. E. Marcucci, Nucl. Phys. A **987**, 1 (2019).

[41] G. X. Dong *et al.*, J. Phys. G Nucl. Partic. **44**, 045201 (2017).

[42] Z.-H. Li *et al.*, Chinese Phys. C **42**, 065001 (2018).

[43] M. Vorabbi *et al.*, Phys. Rev. C **100**, 024304 (2019).

[44] C. Broggini *et al.*, Prog. Part. Nucl. Phys. **98**, 55 (2018).

[45] F. Cavanna and P. Prati, Int. J. Mod. Phys. A **33**, 1843010 (2018).

[46] T. Szücs *et al.*, Eur. Phys. J. A **44**, 513 (2010).

[47] A. Formicola *et al.*, Nucl. Instrum. Methods Phys. Res., Sect. A **507**, 609 (2003).

[48] G. R. Gilmore, *Practical Gamma-ray Spectrometry* (John Wiley & Sons, Weinheim, 2008).

[49] A. Formicola *et al.*, Phys. Lett. B **591**, 61 (2004).

[50] G. Gyürky *et al.*, Phys. Rev. C **100**, 015805 (2019).

[51] G. Imbriani *et al.*, Eur. Phys. J. A **25**, 455 (2005).

[52] D. Piatti, *The Study of $^{22}Ne(\alpha,\gamma)^{26}Mg$ and $^6Li(p,\gamma)^7Be$ Reactions at LUNA* (PhD thesis, University of Padova, 2018).

[53] S. Agostinelli *et al.*, Nucl. Instrum. Methods Phys. Res., Sect. A **506**, 250 (2003).

[54] A. Boeltzig *et al.*, J. Phys. G Nucl. Partic. **45**, 025203 (2018).

[55] T. Chillery, *Underground Study at LUNA of Proton-Induced Reactions on $^6Li$ at Astrophysical Energies* (PhD thesis, University of Edinburgh, 2020).

[56] C. G. Bruno *et al.*, Eur. Phys. J. A **51**, 94 (2015).

[57] C. Bruno *et al.*, Phys. Lett. B **790**, 237 (2019).

[58] S. Pommé, Metrologia **52**, S73 (2015).

[59] Z. Switkowski *et al.*, Nucl. Phys. A **331**, 50 (1979).

[60] A. J. Elwyn *et al.*, Phys. Rev. C **20**, 1984 (1979).

[61] See Supplemental Material at [] for plots of adopted angular distribution coefficients as a function of the energy.

[62] C. Rolfs and W. Rodney, *Cauldrons in the Cosmos* (University of Chicago Press, Chicago, 1988).

[63] C. Iliadis, *Nuclear Physics of Stars, 2nd, Revised and Enlarged Edition* (Wiley-VCH, Weinheim, 2015).

[64] C. R. Brune and D. B. Sayre, Nucl. Instrum. Methods Phys. Res., Sect. A **698**, 49 (2013).

[65] J. Cruz, *Experimental Study of proton induced nuclear reactions in $^{6,7}Li$* (PhD thesis, Universidade Nova de Lisboa, 2006).

[66] H. J. Assenbaum, K. Langanke, and C. Rolfs, Z. Phys. A **327**, 461 (1987).

[67] See Supplemental Material at [] for a table with S-factor values from the present experiment.

[68] R. E. Azuma *et al.*, Phys. Rev. C **81**, 045805 (2010).

[69] C. Angulo *et al.*, Nucl. Phys. A **656**, 3 (1999).

[70] J. I. González Hernández *et al.*, Astron. Astrophys. **628**, A111 (2019).

[71] A. Ćiprijanović, Astropart. Phys. **85**, 24 (2016).